

CHEN, L., SHUNLI, W., JIANG, H. and FERNANDEZ, C. 2022. An adaptive fractional-order unscented Kalman filter for li-ion batteries in the energy storage system. *Indian journal of physics* [online], 96(13), pages 3933-3939. Available from: <https://doi.org/10.1007/s12648-022-02314-2>

An adaptive fractional-order unscented Kalman filter for li-ion batteries in the energy storage system.

CHEN, L., SHUNLI, W., JIANG, H. and FERNANDEZ, C.

2022

This version of the article has been accepted for publication, after peer review (when applicable) and is subject to Springer Nature's [AM terms of use](#), but is not the Version of Record and does not reflect post-acceptance improvements, or any corrections. The Version of Record is available online at:

<https://doi.org/10.1007/s12648-022-02314-2>

An adaptive fractional-order unscented Kalman filter for Li-ion batteries in the energy storage system

L Chen¹, W Shunli^{1*}, H Jiang¹ and C Fernandez²

¹School of Information Engineering, Southwest University of Science and Technology, Mianyang 621010, China

²School of Pharmacy and Life Sciences, Robert Gordon University, Aberdeen AB10-7GJ, UK

Abstract:

Accurate estimation of the state of charge (SOC) can prolong the working life and enhance the safety of energy storage system. Considering the influence of noise and parameter changes in the operating environment, an adaptive fractional-order unscented Kalman filter algorithm is introduced to strengthen the accuracy of SOC estimation. To verify the effectiveness and robustness of the algorithm, the simulation is carried out under UDDS complex conditions. The experimental results indicate that the proposed algorithm has the highest SOC precision among the four algorithms, and the RMSE is 1.37%, indicating the superiority of the fractional-order modeling and the joint estimation algorithm. The online identification of full parameters can solve the shortcoming of the long time to obtain the open-circuit voltage in the experiment, and the adaptive filtering algorithm can overcome the problem of filtering divergence and improve the flexibility of SOC estimation.

Keywords: Li-ion battery; State of charge; Adaptive fractional-order unscented Kalman filter; Energy storage system; Residual sequence

1. Introduction

In the rapid development field of energy storage system, li-ion batteries have been widely applied in the power supply, efficient energy storage, and standby power supply due to the advantages of high energy density, long cycle life, and no pollution [1–3]. The accurate SOC estimation can extend the working life of the energy storage system and improve its safety, which is of great significance to the optimal management of the energy storage system [4, 5]. Since the internal parameters of the battery batteries cannot be measured, it is necessary to establish an equivalent model to simulate the response characteristics of lithium-ion batteries under different working conditions [6, 7]. Li-ion battery equivalent models usually contain three types: black box model, electrochemical mechanism model, and equivalent circuit model (ECM). The ECM describes the operating characteristics of li-ion battery through basic circuit components, which features simple structure and easy to implement [8, 9]. However, Hu et al. [10] proposed that the ideal resistance and capacitance used in traditional ECM cannot adapt to the dynamic characteristics of the battery due to the strong fractional-order characteristics of the actual capacitance. Therefore, the fractional-order model (FOM) based on lithium batteries has attracted more and more attention from scholars [11–13]. Wang et al. [14] developed an iterative search algorithm to identify the parameters of the second-order FOM, and the results fitted the battery model well. Tian et al. [15] compared and verified the voltage response accuracy of the FOM on multiple batteries, and the experimental results showed that the first-order FOM can accurately describe the dynamic response of the battery with fewer parameters. Due to the accuracy of FOM, more and more fractional-order joint Kalman filtering methods are proposed for SOC estimation [16, 17].

Most of the previous SOC estimation methods are offline identification methods based on FOM, which require a long experimental time and low accuracy. The online parameter identification and SOC joint estimation algorithm based on IOM has been implemented [18, 19], while the fractional-order algorithm is rarely implemented. In ref. [20], Tian et al. used the FOM and proposed a method for joint estimation of both online parameter identification and SOC, but they did not consider the noise in the actual environment. In refs. [21, 22], Tian et al. used the least square method to realize online parameter identification, without considering the change of open-circuit voltage in the operating environment.

To characterize the dynamic performance and electrochemical reaction characteristics of the li-ion battery more accurately and improve the adaptability and robustness of the model [23], the dispersion effect, charge-transfer effect between solid electrode/electrolyte interface, and double electron layer effect of the lithium-ion batteries are fully considered, and the constant phase element (CPE) is added to establish the FOM [24, 25]. Considering the influence of noise and parameter changes in the operating environment, an adaptive fractional-order unscented Kalman filter algorithm (AFOUKF) is introduced to strengthen the accuracy of SOC estimation.

2. Mathematical analysis

2.1. Equivalent modeling

Compared with the IOM, the FOM can more accurately characterize the electrochemical effects of li-ion batteries and improve the model accuracy. The ideal voltage source in the FOM is regarded as a controlled current source related to SOC. Such OCV dynamic parameters will change over time, and the proposed model in the whole cycle has higher precision. The improved FOM is shown in Fig. 1.

R_0 is the internal resistance, R_p is the polarization resistance, and CPE is a constant phase element, the fractional-order is expressed as α . U_L is terminal voltage, OCV is a function of SOC, as shown in Eq. (1). An ideal OCV model can be obtained by combining the battery empirical models of Shepherd, Unnewehr and Nernst, where the value K_0 , K_1 , K_2 , K_3 , and K_4 are constants and obtained on the basis of experimental data.

$$U_{OCV} = K_0 - K_1 SOC(k) - K_2 / SOC(k) + K_3 \ln(SOC(k)) + K_4 \ln(1 - SOC(k)) \quad (1)$$

C_1 is the impedance coefficient, S is the variable in the Laplace domain. The impedance form of CPE is defined as shown in Eq. (2). The parallel circuit composed of resistance and CPE represents the resistance and polarization capacitance of the SEI diaphragm, instead of the RC polarization loop in the ECM.

$$Z_{CPE} = \frac{1}{C_1 S^\alpha} \quad (2)$$

Define the differential expression of the SOC expression according to AH integral method, and C_Q denotes the maximum capacity of li-ion battery, η represents the charge-discharge current ratio. According to Kirchhoff's law, the expression of voltage and current of the circuit can be obtained as shown in Eq. (3).

$$\begin{cases} D^1 SOC(t) = -\frac{\eta I(t)}{3600 C_Q} \\ U_L = U_{oc}(SOC) + U_0 + U_p \\ D^\alpha U_p = \frac{I}{C_1} - \frac{U_p}{R_p C_1} \end{cases} \quad (3)$$

Using the definition of the Grunwald–Letnikov fractional derivative, the state space equation is discretized, which can be found in our previous work [26]. The discretized state space format of the FOM can be expressed as shown in Eq. (4).

$$\begin{cases} U_p(k) = \left(a - \frac{T^n}{R_p C_1}\right) U_p(k-1) + \frac{T^n}{C_1} I_{k-1} - \sum_{j=2}^k \binom{a}{j} U_p(k-j) \\ \text{SOC}(k) = \text{SOC}(k-1) + \frac{\eta T}{Q} I_k \\ U_L(k) = U_{OC}(\text{SOC}) - U_p(k) - R_0 I_k \\ U_{OC}(\text{SOC}) = K_0 - K_1 \text{SOC}(k) - K_2 / \text{SOC}(k) \\ \quad + K_3 \ln(\text{SOC}(k)) + K_4 \ln(1 - \text{SOC}(k)) \end{cases} \quad (4)$$

2.2. Parameter identification

The particle swarm optimization is used to identify the offline parameters, and the results are compared with online parameter identification. Each particle updates the local and global optimal values according to the fitness value, and then performs a global optimal search in the solution space. The implementation flow chart is expressed as in Fig. 2. The fitness function is defined as shown in Eq. (5). $U_L(k)$ is the measured voltage, and $U_L(I_k, \hat{\theta})$ is the model terminal voltage. The optimization algorithm is used to identify the parameters in the FOM to minimize the error between $U_L(k)$ and $U_L(I_k, \hat{\theta})$.

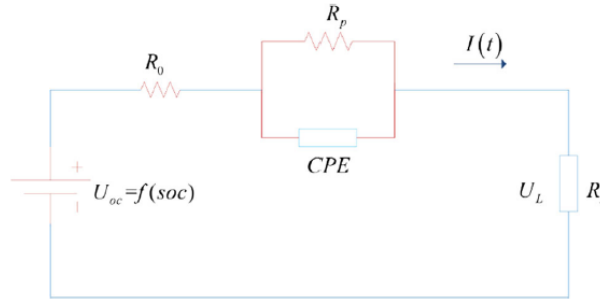


Fig. 1 Fractional-order equivalent circuit model

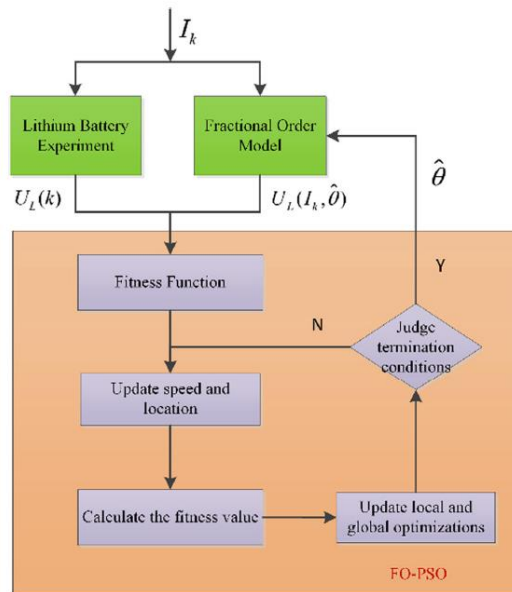


Fig. 2 Parameter identification block diagram of FO-PSO

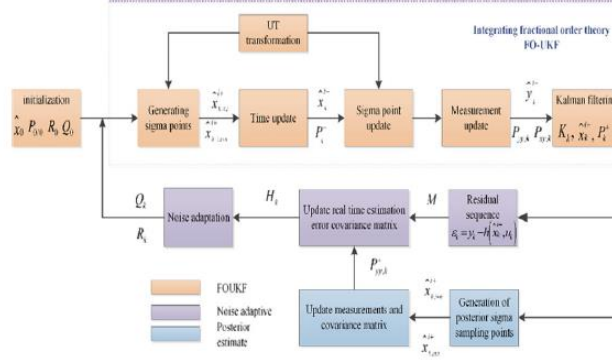


Fig. 3 Flowchart of SOC estimation based on AFOUKF

$$\text{fitness}(\hat{\theta}) = \min_{\hat{\theta}} \sum_{k=1}^N \left(\left| U_L(k) - U_L(I_k, \hat{\theta}) \right| \right) \quad (5)$$

3. A joint estimation method of parameter identification and SOC based on FOM

3.1. Fractional-order unscented Kalman filter algorithm

The FO-UKF algorithm considers the memory effect of the past time of the sample points. Coupled with the optimal estimate of the previous state, the estimated state vector contains some statistical information about the past time. Therefore, FOUKF can estimate the current state of the system more accurately than UKF.

The Kalman filter method can provide a reliable posterior state estimation when the prior statistical values of process noise and measurement noise are known. The covariance matching technique based on the residual sequence can maintain the positive definiteness of the covariance matrix and prevent the filter from diverging. An AFOUKF algorithm based on residual sequence for SOC estimation is proposed in Fig. 3.

The residual sequence ε_k is the difference between the input measurement value y_k and the posterior measurement value $h(x_{k|k}, u_k)$, as shown in Eq. (6).

$$\varepsilon_k = y_k - h(\hat{x}_{k|k}, u_k) \quad (6)$$

H_k is the covariance matrix of the residual sequence at time k , which is the average value of the covariance of the cumulative residual sequence with the size of the sliding window M , as shown in Eq. (7).

$$H_k = \frac{1}{M} \sum_{i=k-M+1}^k \varepsilon_i \varepsilon_i^T \quad (7)$$

According to Eq. (8), the process noise R_k and measurement noise Q_k are calculated to ensure the positive definiteness of the matrix. P_k^{yy+} is the covariance matrix calculated from the sigma sampling points of the posterior estimation, as shown in Eq. (9).

$$R_k = H_k + P_k^{yy+} \quad (8)$$

$$Q_k = KH_kK^T$$

$$P_k^{yy+} = \sum_{i=0}^{2n} \omega_i^c \left[y_{k|k}^i - \hat{y}_{k|k} \right] \left[y_{k|k}^i - \hat{y}_{k|k} \right]^T \quad (9)$$

where $\hat{y}_{k|k} = \sum_{i=0}^{2n} \omega_i^m y_{k|k}^i$, $y_{k|k}^i = h(x_{k|k}^i, u_k)$, $x_{k|k}^i$ is the sigma point generated from FOUKF posterior estimation. The summary of the AFOUKF algorithm is shown in Table 1.

Table 1 Summary of the AFOUKF algorithm

Initialization:

$$\hat{x}_0 = E(x_0) \quad P_{0/0} = E[(x - \hat{x}_0)(x - \hat{x}_0)^T]$$

(a) Compute sigma points

$$\begin{cases} \hat{x}_{k|k-1}^0 = \hat{x}_{k-1} & i = 0 \\ \hat{x}_{k|k-1}^i = \hat{x}_{k-1} + (\sqrt{(n+\kappa)P_{k-1}})_i & i = 1, \dots, n \\ \hat{x}_{k|k-1}^i = \hat{x}_{k-1} - (\sqrt{(n+\kappa)P_{k-1}})_i & i = n+1, \dots, 2n \end{cases}$$

(b) Time update

$$\hat{x}_{k|k-1}^i = f(\hat{x}_{k-1|k-1}^i, u_{k-1})$$

(c) Prior estimation

$$\hat{x}_{k|k-1} = \sum_{i=0}^{2n} \omega_i^m \hat{x}_{k|k-1}^i - \sum_{j=1}^k K_j \hat{x}_{k-j}$$

$$\begin{aligned} P_{xx,k|k-1} &= E\left[\left(\hat{x}_{k|k-1} - \hat{x}_{k|k-1}\right)\left(\hat{x}_{k|k-1} - \hat{x}_{k|k-1}\right)^T\right] + Q_k = E\left[\left(f\left(\hat{x}_{k-1|k-1}^{(i)}, u_{k-1}\right) - \sum_{i=0}^{2n} \omega_i^m \hat{x}_{k|k-1}^i\right) \cdot \left(f\left(\hat{x}_{k-1|k-1}^{(i)}, u_{k-1}\right) - \sum_{i=0}^{2n} \omega_i^m \hat{x}_{k|k-1}^i\right)^T\right] \\ &+ \left(\sum_{j=1}^k K_j \hat{x}_{k-j}\right)^T E\left[\left(f\left(\hat{x}_{k-1|k-1}^{(i)}, u_{k-1}\right) - \sum_{i=0}^{2n} \omega_i^m \hat{x}_{k|k-1}^i\right)\right] + \sum_{j=1}^k K_j \hat{x}_{k-j} E\left[\left(f\left(\hat{x}_{k-1|k-1}^{(i)}, u_{k-1}\right) - \sum_{i=0}^{2n} \omega_i^m \hat{x}_{k|k-1}^i\right)^T\right] \\ &+ \sum_{j=1}^k K_j \hat{x}_{k-j} \left(\hat{x}_{k-j}\right)^T + Q_{k-1} \end{aligned}$$

(d) Updates sigma points

(e) Measurement update

$$\begin{cases} \hat{y}_{k|k-1}^i = h\left(\hat{x}_{k|k-1}^i, u_k\right) \\ \hat{y}_{k|k-1} = \sum_{i=0}^{2n} \omega_i^m \hat{y}_{k|k-1}^i \\ \begin{cases} P_{yy,k} = \sum_{i=0}^{2n} \omega_i^m \left[\hat{y}_{k|k-1}^i - \hat{y}_{k|k-1}\right] \left[\hat{y}_{k|k-1}^i - \hat{y}_{k|k-1}\right]^T + R_{k-1} \\ P_{xy,k} = \sum_{i=0}^{2n} \omega_i^m \left[\hat{x}_{k|k-1}^i - \hat{x}_{k|k-1}\right] \left[\hat{y}_{k|k-1}^i - \hat{y}_{k|k-1}\right]^T \end{cases} \end{cases}$$

(f) Posterior estimate

$$K_k = P_{xy,k} / P_{yy,k}$$

$$e_k = y_k - \hat{y}_{k|k-1}$$

$$\hat{x}_{k|k} = \hat{x}_{k|k-1} + K_k e_k$$

$$P_{xx,k|k} = P_{xx,k|k-1} - K_k P_{yy,k} K_k^T$$

(g) Calculate the residuals sequence and real-time estimation of the covariance matrix

$$z_k = y_k - h(\hat{x}_{k|k}, u_k)$$

$$H_k = \frac{1}{M} \sum_{i=k-M+1}^k z_i z_i^T$$

(h) Generate the posterior sigma points

$$\begin{cases} \hat{x}_{k|k}^i = \left[\hat{x}_{k|k} \quad \hat{x}_{k|k} + (\sqrt{(n+\kappa)P_{xx,k|k}})_i \quad \hat{x}_{k|k} - (\sqrt{(n+\kappa)P_{xx,k|k}})_i\right] \\ \begin{cases} \hat{y}_{k|k}^i = h\left(\hat{x}_{k|k}^i, u_k\right) \\ \hat{y}_{k|k} = \sum_{i=0}^{2n} \omega_i^m \hat{y}_{k|k}^i \end{cases} \end{cases}$$

$$P_k^{pp} = \sum_{i=0}^{2n} \omega_i^m \left[\hat{y}_{k|k}^i - \hat{y}_{k|k}\right] \left[\hat{y}_{k|k}^i - \hat{y}_{k|k}\right]^T$$

(i) Adaptive noise update

$$R_k = H_k + P_k^{pp}$$

$$Q_k = KH_kK^T$$

3.2. A joint estimation method of full-parameter identification and SOC based on FOM

The parameters of the li-ion battery model are affected by factors such as SOC, ambient temperature, and battery aging, and they are closely related to the working state of the battery. With the battery charge and discharge cycles, the SOC value and internal resistance have been changed. Therefore, the battery model parameters need to be identified online and updated in real time to ensure the accuracy of the battery model. A joint estimation method of parameter identification and SOC based on FOM is introduced. The algorithm is based on FFRLS to realize full-parameter online identification, and the AFOUKF algorithm is used to realize SOC estimation. The flowchart of the joint estimation method of full-parameter identification and SOC is expressed as in Fig. 4.

The combined method can both improve the accuracy of the battery model and the accuracy of the SOC. The noise adaptive algorithm based on residual sequence is applied to improve the convergence speed of the algorithm.

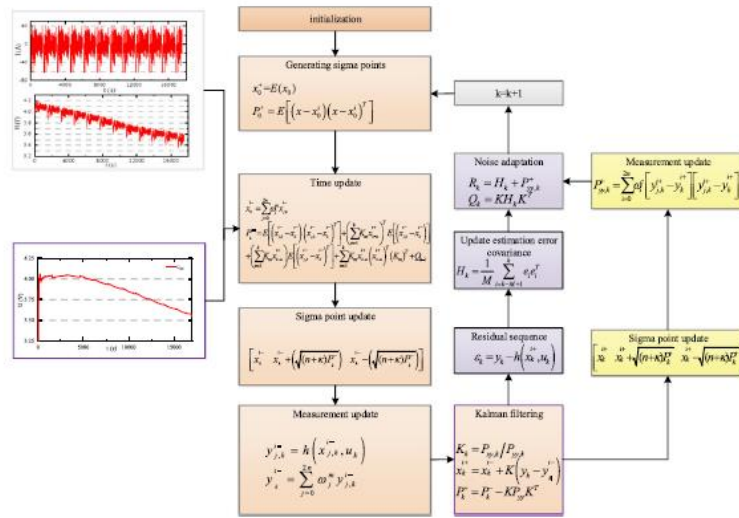


Fig. 4 Flowchart of the proposed algorithm

4. Experimental analysis

4.1. Experimental working conditions

The lithium iron phosphate battery is selected as the experimental object. The entire battery test bench is shown in Fig. 5.

The experimental equipment includes battery test equipment, a temperature chamber and a host computer. Figure 6a and b shows the dynamic current and voltage curves during the urban dynamometer driving schedule (UDDS) test.

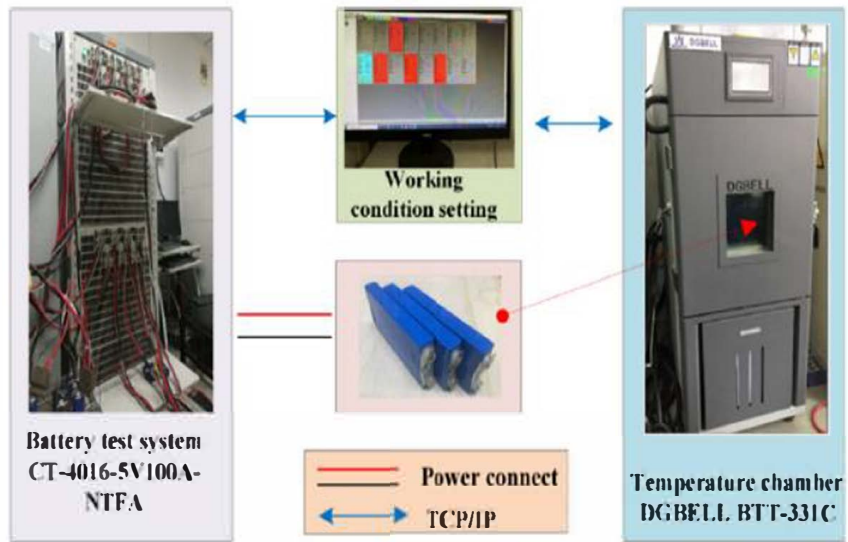
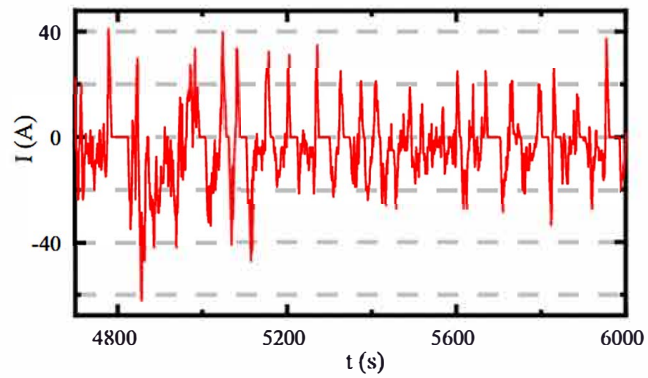
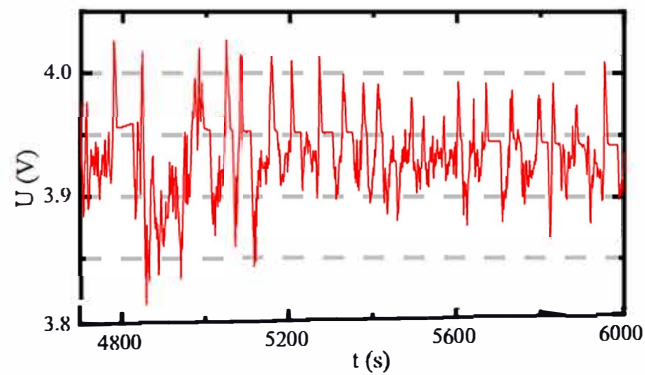


Fig. 5 Entire battery test bench



(a) dynamic current profile



(b) Voltage profiles

Fig. 6 UDDS test

4.2. Parameter identification results

The PSO is used to identify the parameters, and the number of iterations is set to 3000. The offline parameter identification results are shown in Fig. 7. Figure 7a–d, respectively, represents the identification results of fractional order a , ohmic internal resistance, constant phase element, and polarization internal resistance.

4.3. SOC estimation results

The UDDS data are selected to verify the performance of the joint estimate method. The RMSE, MAE, and MAPE are selected to evaluate the model and state estimation results.

Different parameter identification methods are used to verify the accuracy of IOM and FOM in SOC estimation. The comparison values are shown in Table 2.

The proposed AFOUKF_ON algorithm is a joint estimation algorithm that combines fractional-order theory, residual adaptive filtering and full-parameter online identification. The experimental results prove that the algorithm has the highest estimation accuracy, and its RMSE, MAPE, and MAE are 1.37, 3.53, and 1.11%, respectively.

The SOC estimation results and error comparison are shown in Fig. 8a and b. The voltage comparison and error comparison are shown in Fig. 8c and d. Figure 8a and b shows that due to the adaptive update of noise covariance, the filter can quickly converge the wrong SOC initial value under four different methods, which ensures the accuracy of the SOC estimation result. The SOC estimation results based on full-parameter identification are better than offline identification in both FOM and IOM.

The results show that the online update of full parameters can improve the accuracy of SOC estimation, especially in the case of large errors at the beginning and end of the cycle. The errors of the three evaluation indexes of FOM are all lower than IOM, indicating that the introduction of fractional-order can better describe the dynamic characteristics of the battery, and the accuracy of the model has been significantly improved. The online full-parameter identification can significantly reduce the influence of noise, achieve higher accuracy and faster convergence speed, and ensure the convergence and stability of the algorithm.

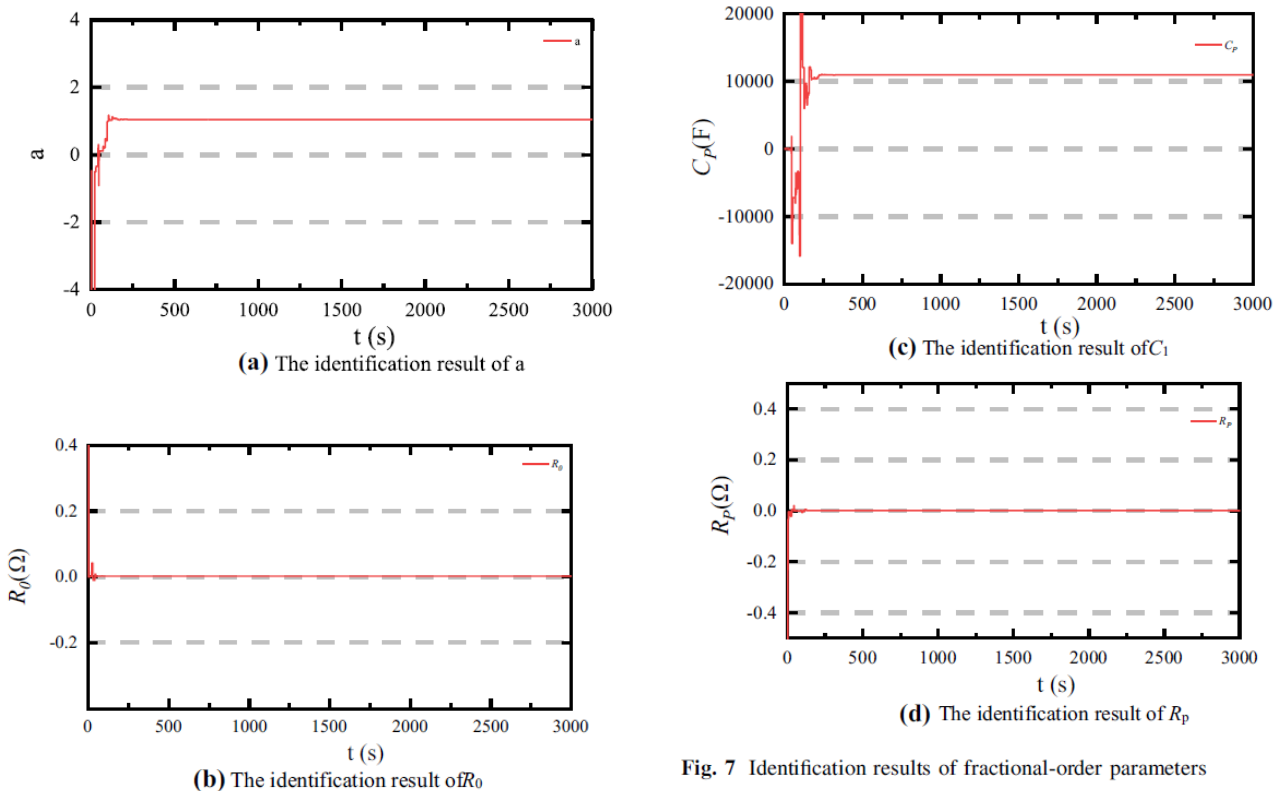
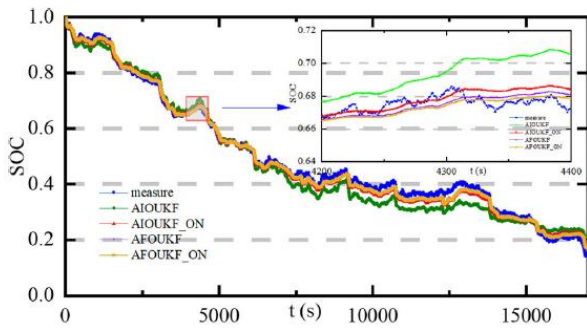
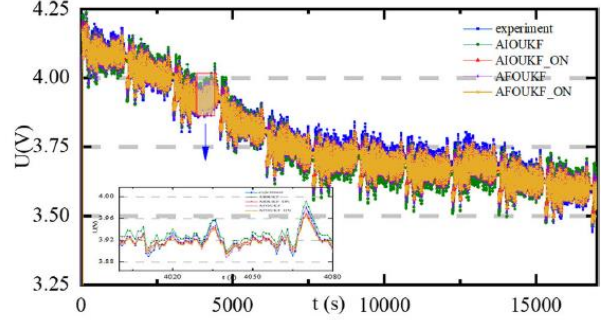


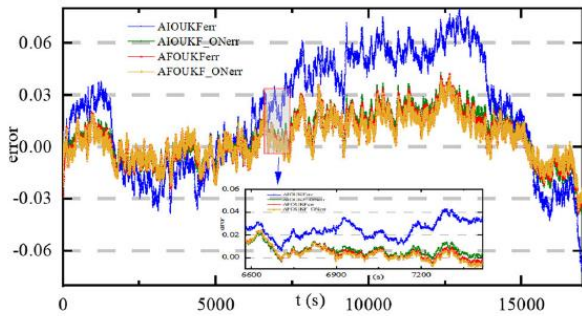
Fig. 7 Identification results of fractional-order parameters



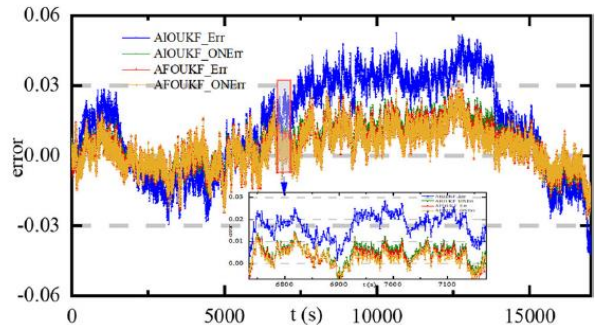
(a) Comparison of SOC based on two algorithms



(c) Comparison of voltage based on two algorithms



(b) Comparison of SOC error based on two algorithms



(d) Comparison of voltage error based on two algorithms

Fig. 8 Performance comparison based on two algorithms

The proposed AFOUKF_ON algorithm is a joint estimation algorithm that combines fractional-order theory, residual adaptive filtering and full-parameter online identification. The experimental results prove that the algorithm has the highest estimation accuracy, and its RMSE, MAPE, and MAE are 1.37, 3.53, and 1.11%, respectively.

The SOC estimation results and error comparison are shown in Fig. 8a and b. The voltage comparison and error comparison are shown in Fig. 8c and d. Figure 8a and b shows that due to the adaptive update of noise covariance, the filter can quickly converge the wrong SOC initial value under four different methods, which ensures the accuracy of the SOC estimation result. The SOC estimation results based on full-parameter identification are better than offline identification in both FOM and IOM.

The results show that the online update of full parameters can improve the accuracy of SOC estimation, especially in the case of large errors at the beginning and end of the cycle. The errors of the three evaluation indexes of FOM are all lower than IOM, indicating that the introduction of fractional-order can better describe the dynamic characteristics of the battery, and the accuracy of the model has been significantly improved. The online full-parameter identification can significantly reduce the influence of noise, achieve higher accuracy and faster convergence speed, and ensure the convergence and stability of the algorithm.

Table 2 Performance comparison of four algorithms under different parameter identification

	AIOUKF	AFOUKF	AIOUKF_ON	AFOUKF_ON
RMSE	3.93%	1.49%	1.67%	1.37%
MAPE	9.85%	3.66%	4.23%	3.53%
MAE	3.35%	1.22%	1.38%	1.11%

5. Conclusions

A joint algorithm of online full-parameter identification and SOC estimation is introduced. FFRLS is used to complete online parameter identification, which improves the accuracy of full-cycle identification and overcomes the disadvantage of a long time to obtain OCV value. The AFOUKF algorithm is applied to complete the SOC estimation, which overcomes the problem of filtering divergence and improves the flexibility of SOC estimation.

Compared with the IOM, the FOM can characterize the electrochemical effects of li-ion batteries more accurately and improve the accuracy of the model. The experimental results indicate that the combined algorithm can update the model parameters in real time, which can both improve the accuracy of the battery model and the stability and robustness of the SOC.

Acknowledgements: The work is supported by the National Natural Science Foundation of China (No. 61801407), Sichuan science and technology program (No. 2019YFG0427), China Scholarship Council (No. 201908515099).

References

- [1] T Sun, B Xia, Y Liu, Y Lai, W Zheng, H Wang, W Wang and M Wang, *Energies*, 12 (2019)
- [2] Y Tian, D Li, J Tian and B Xia *Electrochim. Acta* 225 225 (2017)
- [3] B Xia, R Huang, Z Lao, R Zhang, Y Lai, W Zheng, H Wang, W Wang and M Wang, *Energies*, 11 (2018)
- [4] B Xia, Z Sun, R Zhang and Z Lao, *Energies*, 10 (2017)
- [5] C Liu, Y Wang and Z Chen *Energy* 166 796 (2019)
- [6] K Zhang, J Ma, X Zhao, D Zhang and Y He, *IEEE Access*, 7 (2019) 166657
- [7] X Hu, H Yuan, C Zou, Z Li and L Zhang *IEEE Trans. Veh. Technol.* 67 10319 (2018)
- [8] L Zhang, H Peng, Z Ning, Z Mu and C Sun *Appl. Sci.* 7 1002 (2017)
- [9] Y Sun, Y Li, M Yu, Z Zhou, Q Zhang, B Duan, Y Shang and C Zhang, *J. Power Sources*, 448 (2020)
- [10] M Hu, Y Li, S Li, C Fu, D Qin and Z Li *Energy* 165 153 (2018)
- [11] G Jin, L Li, Y Xu, M Hu, C Fu and D Qin, *Energies*, 13 (2020)
- [12] L Li, H Zhu, A Zhou, M Hu, C Fu and D Qin *Int. J. Electrochem. Sci.* 15 6863 (2020)
- [13] S Liu, X Dong and Y Zhang *IEEE Access*. 7 122949 (2019)
- [14] Y Wang, G Gao, X Li and Z Chen *J. Power Sources*.449 227543 (2020)
- [15] J Tian, R Xiong, W Shen and J Wang, *Chinese Journal of Mechanical Engineering*, 33 (2020)
- [16] Q Zhang, Y Shang, Y Li, N Cui, B Duan and C Zhang *ISA Trans*